Aeroelastic Analysis of Bridges: Effects of Turbulence and Aerodynamic Nonlinearities

Xinzhong Chen[1] and Ahsan Kareem[2]

Abstract: Current linear aeroelastic analysis approaches are not suited for capturing the emerging concerns in bridge aerodynamics introduced by aerodynamic nonlinearities and turbulence effects. These issues may become critical for bridges with increasing spans and/or with aerodynamic characteristics sensitive to the effective angle of incidence. This paper presents a nonlinear aerodynamic force model and associated time domain analysis framework for predicting the aeroelastic response of bridges under turbulent winds. The nonlinear force model separates the aerodynamic force into low- and high-frequency components according to the effective angle of incidence. The low-frequency force component is modeled utilizing quasi-steady theory. The high-frequency force component is based on the frequency dependent unsteady aerodynamic characteristics, which are similar to the traditional force model but vary in space and time following the low-frequency effective angle of incidence. The proposed framework provides an effective analysis tool to study the influence of structural and aerodynamic nonlinearities and turbulence on the bridge aeroelastic response. The effectiveness of this approach is demonstrated by utilizing an example of a long span suspension bridge with aerodynamic characteristics sensitive to the angle of incidence. The influence of mean wind angle of incidence on the aeroelastic modal properties and the associated aeroelastic response and the sensitivity of bridge response to nonlinear aerodynamics and low-frequency turbulence are examined.

DOI: 10.1061/(ASCE)0733-9399(2003)129:8(885)

CE Database subject headings: Flutter; Buffeting; Turbulence; Bridges; Wind forces; Aerodynamics.

Introduction

The aerodynamic performance under the action of strong winds is of major concern because it serves as a governing criterion for the design and construction of long span bridges. The understanding of aeroelastic response of bridges has been significantly improved through experimental and analytical studies. Remarkable developments in analytical approaches have been made since the pioneering studies by Davenport (1962) and Scanlan (1978) among others. These analytical approaches utilize aerodynamic forces linearized at the statically deformed position of the bridge, which are commonly separated into static, self-excited, and buffeting force components. Advances in identifying force parameters such as static force coefficients, flutter derivatives, aerodynamic admittance functions, and spanwise coherence functions, utilizing scaled bridge models in wind tunnels have led to remarkable improvements in accurately modeling aerodynamic forces and predicting the overall aeroelastic response of bridges (Walshe and Wyatt 1983; Davenport et al. 1992; Scanlan 1993; Sakar et al. 1994; Larose and Mann 1998; Chen and Kareem 2002). In conjunction with experimentally identified force parameters, analytical approaches have been widely used in the design of many bridges. Conventional analytical techniques, which rely on the assumption that intermodal coupling is negligible and flutter is dominated by a single torsional mode, have adequately predicted the response of typical cable supported bridges built thus far. However, experience shows that this may not be a valid assumption for exceptionally long span bridges which require a multimode coupled analysis framework (e.g., Miyata et al. 1995; Jones et al. 1998; Katsuchi et al. 1999; Chen et al. 2000a; Xu et al. 2000; Chen et al. 2001).

Aeroelastic analyses have been predominantly conducted in the frequency domain because it facilitates the modeling of frequency dependent characteristics of unsteady aerodynamic forces. However, it is constrained by the assumptions of linearity in both structural dynamics and aerodynamics, and stationarity of wind fluctuations. Challenges in analytical approaches remain in the areas of modeling aerodynamic forces excited by nonstationary wind fields such as hurricanes and thunderstorms, for bridges located in complex topography (Davenport and King 1993), consideration of nonlinearities in both structural dynamics and aerodynamics, and ubiquitous issues related to turbulence. Clearly, these challenges can only be adequately addressed in a time or time-frequency domain analysis framework.

Most of the previous studies concerning time domain analysis of buffeting response were based on quasi-steady aerodynamic forces due to their inability to model frequency dependent unsteady aerodynamic characteristics in the time domain (e.g., Kovacs et al. 1992; Miyata et al. 1995). Therefore, its application should be limited to those cases where reduced velocity is sufficiently high such that the unsteady fluid memory effect may be ignored. Chen et al. (2000b) proposed a time domain analysis framework in which frequency dependent aerodynamic forces can

[1]Postdoctoral Research Associate, Dept. of Civil Engineering and Geological Sciences, Univ. of Notre Dame, Notre Dame, IN 46556. E-mail: xchen@nd.edu

[2]Robert M. Moran Professor, Dept. of Civil Engineering and Geological Sciences, Univ. of Notre Dame, Notre Dame, IN 46556. E-mail: ahsan.kareem.1@nd.edu

Note. Associate Editor: Roger G. Ghanem. Discussion open until January 1, 2004. Separate discussions must be submitted for individual papers. To extend the closing date by one month, a written request must be filed with the ASCE Managing Editor. The manuscript for this paper was submitted for review and possible publication on June 17, 2002; approved on December 16, 2002. This paper is part of the ***Journal of Engineering Mechanics***, Vol. 129, No. 8, August 1, 2003. ©ASCE, ISSN 0733-9399/2003/8-885–895/$18.00.

be modeled akin to the frequency domain approach. An alternative approach utilizing an integrated state-space model was also presented by Chen and Kareem (2001a) in which bridge response under turbulent winds was described as the output of an integrated system driven by a vector-valued white noise. With this state-space model approach, the buffeting response can be directly calculated with higher-computational efficiency using the Lyapunov equation rather then conventional spectral analysis. This integrated state-space approach is particularly well suited for studies of active control of bridge flutter and buffeting responses.

Current linear aerodynamic force models have proven their utility for many applications, however, these are not suited for completely addressing the challenges posed by aerodynamic nonlinearities and turbulence effects. Experimental studies have shown that aerodynamic characteristics of many innovative bridge deck designs, with attractive aerodynamic performance, are very sensitive to the angle of incidence (e.g., Zasso and Curami 1993; Matsumoto et al. 1998). For these bridge sections, even for low levels of turbulence, the effective angle of incidence due to structural motions and incoming wind fluctuations may vary to the extent that the nonlinearities in the aerodynamic forces may no longer be neglected. Current analytical approaches also fall short in predicting the turbulence effects on bridge flutter (Irwin 1977; Scanlan and Lin 1978; Matsumoto 1999).

A number of analytical studies based on randomizing the dynamic pressure and invoking stochastic approaches were conducted to predict some general changes in flutter instability due to incoming turbulence (e.g., Bucher and Lin 1988; and Lin and Li 1993). These studies tacitly assume that the mechanism relating wind field to the aerodynamic forces remains unchanged in turbulent flows. Such an ad hoc implementation of turbulence may not accurately represent the underlying physics because turbulence may indeed significantly modify the flow structure, attendant aerodynamics, and resulting forces (Nakamura 1993). Scanlan (1997) explored the potential mechanism of turbulence on the single-mode torsional flutter due to a decrease in spanwise correlation of the self-excited forces. Although the stabilizing effect of spanwise correlation loss may be apparent for single-mode torsional flutter, it is not obvious that this will indeed apply to multimode coupled flutter cases. Correlation loss along the span may stabilize a bridge by reducing unfavorable negative aerodynamic damping effects, but it may destabilize a bridge by reducing favorable aerodynamic damping. This issue will become even more important as the bridge span lengthens and the potential for multimode flutter increases. A recent experimental study demonstrated the near unity coherence of self-excited forces in several turbulent flows (Haan et al. 2000). This tends to support full correlation of the self-excited forces implied in current analytical approaches. However, this also implies that the turbulence-induced changes in flutter instability of bridges cannot be explained entirely due to a decrease in the coherence of self-excited forces.

Diana et al. (1995 and 1999) proposed a nonlinear aerodynamic force model based on so-called ''quasi-static corrected theory'' and analytically investigated turbulence effects on flutter and buffeting responses. This nonlinear force model attempted to incorporate frequency dependent characteristics by decomposing the total response into components with different frequencies. A novel nonlinear aerodynamic force model and associated time domain analysis framework have been proposed by Chen and Kareem (2001b). This nonlinear aerodynamic force model incorporates nonlinear and unsteady features based on the static force coefficients, flutter derivatives, and admittance functions along with the spanwise correlations at varying angles of incidence. It offers a clear relationship with current linear unsteady force and nonlinear quasi-steady force models. The proposed framework provides an innovative tool to study the influence of structural and aerodynamic nonlinearities and turbulence on aeroelastic response of bridges.

In this paper, a detailed presentation of the nonlinear aerodynamic force model and associated time domain analysis framework originally introduced in Chen and Kareem (2001b) is outlined for predicting the aeroelastic response of bridges under turbulent winds. A new application of this framework to a long span suspension bridge, with aerodynamic characteristics that are very sensitive to the angle of incidence, is provided to further examine the influence of mean wind angle of incidence on the aeroelastic modal properties and aeroelastic response based on linear aerodynamic forces. It also explores the influence of nonlinear aerodynamics and low-frequency turbulence on the bridge aeroelastic response.

Nonlinear Aerodynamic Forces

The traditional linear aerodynamic force model tacitly assumes that the variations of an effective angle of incidence are sufficiently small such that the corresponding changes in aerodynamic characteristics can be neglected and assumes the value at the statically deformed position of the bridge. For some bridge sections whose aerodynamic characteristics are highly sensitive to the changes in the mean angle of incidence, the nonlinearities in the aerodynamic forces may not be neglected depending on their sensitivity and the range of variation of the effective angle of incidence. While the quasi-steady force model can take into account the nonlinearities in aerodynamic forces through the static force coefficients, which are nonlinear functions of the angle of incidence, it discards the unsteady fluid memory effect which results in frequency dependent attenuation and phase delays of the aerodynamic forces with respect to the quasi-steady results. The quasi-steady assumption is only considered valid at very high-reduced wind velocities. It fails in accurately describing forces at low-wind velocities and forces induced by torsional motion even at very high-reduced velocities, in which the fluid memory effect plays an essential role in force generation (e.g., van Oudheusden 2000).

In principle, the nonlinear aerodynamic forces can be generally expressed as a function of the effective angle of incidence α_e with corresponding force coefficients. The effective angle of incidence is a function of structural motion and incoming wind fluctuations, which can be clearly formulated for quasi-steady aerodynamic forces but not in a straightforward manner for the unsteady cases. In Diana et al. (1995 and 1999), different effective angles of incidence for lift and pitching moment components of the unsteady aerodynamic forces were suggested for a nonlinear force model.

In this study, in order to model the nonlinear aerodynamic forces, the effective angle of incidence is separated into low-frequency (large length scale) and high-frequency (small length scale) components

$$\alpha_e(t) = \alpha_e^l(t) + \alpha_e^h(t) \tag{1}$$

where superscripts l and h indicate the low-frequency (including static component) and high-frequency components. The low- and high-frequency ranges are separated at a critical frequency. The selection of this critical frequency warrants an in-depth examina-

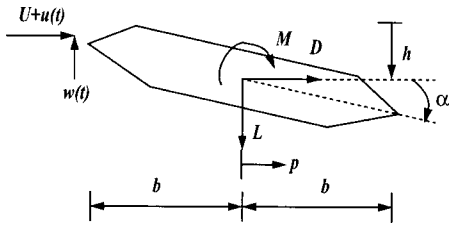

Fig. 1. Coordinate system for analysis

tion, however, in this study it is assumed to be the first natural frequency of the bridge. The low-frequency turbulence is modeled to introduce changes in the mean angle of incidence which influence bridge aerodynamics. The high-frequency turbulence is modeled to alter the flow structure around the bridge section. Hence the aerodynamics and the resulting forces can be modeled by directly using the aerodynamic characteristics measured in turbulent flow conditions. Accordingly, the nonlinear aerodynamic forces are approximately expressed in terms of the sum of the low- and high-frequency components

$$\mathbf{F}=\mathbf{F}(\alpha_e)\approx\mathbf{F}(\alpha_e^l)+\left.\frac{d\mathbf{F}}{d\alpha}\right|_{\alpha_e^l}\alpha_e^h=\mathbf{F}^l+\mathbf{F}_{se}^h+\mathbf{F}_b^h \tag{2}$$

The low-frequency force component (including the static force component) is expressed as a nonlinear function of the effective angle of incidence $\alpha_e^l(t)$ in light of the quasi-steady theory as follows (Fig. 1):

$$L^l=F_L^l\cos\phi^l-F_D^l\sin\phi^l;\quad D^l=F_L^l\sin\phi^l+F_D^l\cos\phi^l;$$
$$M^l=F_M^l \tag{3}$$

$$F_L^l=-\tfrac{1}{2}\rho V_r^2BlC_L(\alpha_e^l);\quad F_D^l=\tfrac{1}{2}\rho V_r^2BlC_D(\alpha_e^l);$$
$$F_M^l=\tfrac{1}{2}\rho V_r^2B^2lC_M(\alpha_e^l) \tag{4}$$

$$V_r^2=(U+u^l-\dot{p}^l)^2+(w^l+\dot{h}^l+m_1b\dot{\alpha}^l)^2 \tag{5}$$

$$\alpha_e^l=\alpha_s+\phi^l;\quad \phi^l=\arctan\left(\frac{w^l+\dot{h}^l+m_1b\dot{\alpha}^l}{U+u^l-\dot{p}^l}\right) \tag{6}$$

where ρ=air density; U=mean wind velocity; $B=2b$=bridge deck width; C_L, C_D, and C_M=mean lift, drag, and pitching moment coefficients, respectively; α_s=time-averaged static angle of the bridge section; u^l and w^l=longitudinal and vertical wind fluctuations; $h^l(t)$, $p^l(t)$, and $\alpha^l(t)$=low-frequency components of the dynamic displacements in the vertical, lateral, and torsional directions, respectively; α_e=effective angle of incidence; m_1 is assumed to be 0.5; and the over dot denotes the derivative with respect to time.

The utility of the quasi-steady theory for modeling the low-frequency force component is due to its validity at high-reduced velocities. When the low-frequency dynamic response is comparatively small and negligible as is the case for most long-span bridges, α_e^l is simplified as

$$\alpha_e^l=\alpha_s+\arctan\left(\frac{w^l}{U+u^l}\right) \tag{7}$$

The high-frequency components of the aerodynamic forces are then expressed by a linearization around the low-frequency effective angle of attack $\alpha_e^l(t)$. They can be further separated into self-excited and buffeting force components as in the case of linear aerodynamic forces. Assuming that the self-excited forces within an element are spatially fully correlated, the linearized self-excited forces acting on an element undergoing arbitrary structural motions can be given in terms of a convolution integral for the lift component (e.g., Chen et al. 2000b):

$$L_{se}^h(t)=\frac{1}{2}\rho U^2l\int_{-\infty}^{t}(I_{Lh}(\alpha_e^l,t-\tau)h^h(\tau)+I_{Lp}(\alpha_e^lt-\tau)p^h(\tau)$$
$$+I_{L\alpha}(\alpha_e^l,t-\tau)\alpha^h(\tau))d\tau \tag{8}$$

where $h^h(t)$, $p^h(t)$, and $\alpha^h(t)$=high-frequency components of the dynamic displacements in the vertical, lateral, and torsional directions, respectively; I_{Lh}, I_{Lp}, and $I_{L\alpha}$=aerodynamic impulse response functions; and l=element length. Unlike the airfoil section in which these aerodynamic impulse functions are related to the Wagner function, bluff bridge sections generally require the use of different functions for different force components associated with the lateral, vertical, and torsional motions. Analogous formulations exist for the drag and moment components.

The spatial correlation of the buffeting forces should also be considered in these calculations, which leads to a reduction in the overall forces. While it is commonly assumed, based on the strip theory, that the buffeting forces have the same spatial correlation as the fluctuations in the approach wind, measurements have otherwise suggested that the pressure field may have a higher-spanwise correlation (e.g., Davenport et al. 1992; Larose and Mann 1998). The linearized buffeting forces acting on an element corresponding to arbitrary wind fluctuations can be given in terms of a convolution integral for the lift component (Chen et al. 2000b):

$$L_b^h(t)=-\frac{1}{2}\rho U^2l\int_{-\infty}^{t}\int_{-\infty}^{\tau_2}\Bigg(J_{Lu}(\alpha_e^l,t-\tau_2)$$
$$\times I_{Lu}(\alpha_e^l,\tau_2-\tau_1)\frac{u^h(\tau_1)}{U}$$
$$+J_{Lw}(\alpha_e^l,t-\tau_2)I_{Lw}(\alpha_e^l,\tau_2-\tau_1)\frac{w^h(\tau_1)}{U}\Bigg)d\tau_1d\tau_2 \tag{9}$$

where u^h and w^h=wind fluctuations at the center of the element in the longitudinal and vertical directions, respectively; I_{Lu} and I_{Lw}=aerodynamic impulse response functions of buffeting forces representing the unsteady characteristics of buffeting forces on unit length; and J_{Lu} and J_{Lw} indicate the impulse response functions representing the spatial correlation characteristics. Similar expressions exist for the drag and moment components.

For sinusoidal structural motions and wind fluctuations, the lift components of the self-excited and buffeting forces are commonly expressed in terms of flutter derivatives, admittance functions and joint acceptance functions as

$$L_{se}^h(t)=\frac{1}{2}\rho U^2Bl\Bigg(kH_1^*\frac{\dot{h}}{U}+kH_2^*\frac{b\dot{\alpha}}{U}+k^2H_3^*\alpha+k^2H_4^*\frac{h}{b}$$
$$+kH_5^*\frac{\dot{p}}{U}+k^2H_6^*\frac{p}{b}\Bigg) \tag{10}$$

$$L_b^h(t)=-\frac{1}{2}\rho U^2Bl\left(2C_L\overline{J}_{Lu}\chi_{Lu}\frac{u}{U}+(C_L'+C_D)\overline{J}_{Lw}\chi_{Lw}\frac{w}{U}\right) \tag{11}$$

where $k=\omega b/U$=reduced frequency; ω=circular frequency of

vibration; H_i^* $(i=1,2,\ldots,6)$=frequency dependent flutter derivatives; χ_{Lu} and χ_{Lw} denote the aerodynamic transfer functions between fluctuating wind velocities and buffeting forces per unit span (the absolute magnitude of these functions are also referred to as aerodynamic admittance functions); $\overline{J_{Lu}}$ and $\overline{J_{Lw}}$ represent the joint acceptance functions and are the Fourier transforms of the respective impulse response functions J_{Lu} and J_{Lw}.

The relationship between the aerodynamic impulse response functions, flutter derivatives, and admittance functions are given as (Chen et al. 2000b):

$$\overline{I_{Lh}}=2k^2(H_4^*+iH_1^*); \quad \overline{I_{Lp}}=2k^2(H_6^*+iH_5^*);$$
$$\overline{I_{L\alpha}}=2k^2b(H_3^*+iH_2^*) \tag{12}$$

$$\overline{I_{Lu}}=4bC_L\chi_{Lu}; \quad \overline{I_{Lw}}=2b(C_L'+C_D)\chi_{Lw} \tag{13}$$

where the over bar denotes the Fourier transform operator, and $i=\sqrt{-1}$.

The joint acceptance functions are related to the coherence function coh_r as

$$\overline{J_r^2}=\frac{1}{l^2}\int_0^l\int_0^l \mathrm{coh}_r(x_1,x_2;f)dx_1dx_2 \quad (r=Lu,Lw) \tag{14}$$

where x_1 and x_2=spatial coordinates.

The aerodynamic impulse response functions can be expressed in terms of exponential time-series approximations. For the functions relevant to the self-excited forces, aerodynamic damping and inertia terms can also be included. For example, $I_{Lh}(t)$ is expressed as

$$I_{Lh}(t)=\left(A_{Lh,1}+\sum_{j=1}^{m_{Lh}}A_{Lh,j+3}\right)\delta(t)+A_{Lh,2}\frac{b}{U}\dot{\delta}(t)+A_{Lh,3}\frac{b^2}{U^2}\ddot{\delta}(t)$$
$$-\sum_{j=1}^{m_{Lh}}A_{Lh,j+3}\frac{d_{Lh,j}U}{b}\exp\left(-\frac{d_{Lh,j}U}{b}t\right) \tag{15}$$

and for the functions relevant to buffeting forces, for example, $I_{Lw}(t)$ is expressed as

$$I_{Lw}(t)=2b(C_L'+C_D)\left[\left(A_{Lw,1}+\sum_{j=1}^{m_{Lw}}A_{Lw,j+3}\right)\delta(t)\right.$$
$$\left.-\sum_{j=1}^{m_{Lw}}A_{Lw,j+1}\frac{d_{Lw,j}U}{b}\exp\left(-\frac{d_{Lw,j}U}{b}t\right)\right] \tag{16}$$

where $A_{Lh,1}$, $A_{Lh,2}$, $A_{Lh,3}$, $A_{Lh,j+3}$, and $d_{Lh,j}$ $(d_{Lh,j}\geqslant 0;$ $j=1,2,\ldots,m_{Lh})$ and $A_{Lw,1}$ and $d_{Lw,j}$ $(d_{Lw,j}\geqslant 0;$ $j=1,2,\ldots,m_{Lw})$=frequency independent coefficients and are functions of the angle of incidence. These coefficients can be quantified by fitting the flutter derivatives and admittance function and joint acceptance functions at varying angles of incidence in the frequency domain as follows:

$$2k^2(H_4^*+iH_1^*)=A_{Lh,1}+(ik)A_{Lh,2}+(ik)^2A_{Lh,3}$$
$$+\sum_{j=1}^{m_{Lh}}\frac{(ik)A_{Lh,j+3}}{ik+d_{Lh,j}} \tag{17}$$

$$\chi_{Lw}=A_{Lw,1}+\sum_{j=1}^{m_{Lw}}\frac{(ik)A_{Lw,j+1}}{ik+d_{Lw,j}} \tag{18}$$

Accordingly, the unsteady frequency dependent aerodynamic force, e.g., $L^{\mathrm{seh}}(t)$, is represented in terms of structural motion and augmented aerodynamic states that are governed by a set of first-order differential equations excited by the structural motion

$$L^{\mathrm{seh}}(t)=\frac{1}{2}\rho U^2\left(A_{Lh,1}h^h(t)+A_{Lh,2}\frac{b}{U}\dot{h}^h(t)+A_{Lh,3}\frac{b^2}{U^2}\ddot{h}^h(t)\right.$$
$$\left.+\sum_{j=1}^{m_{Lh}}\phi_j^h(t)\right) \tag{19}$$

$$\dot{\phi}_j^h(t)=-\frac{d_{Lh,j}U}{b}\phi_j^h(t)+A_{Lh,j+3}\dot{h}^h(t) \quad (j=1,2,\ldots,m_{Lh}) \tag{20}$$

where $\phi_j^h(t)$ $(j=1,2,\ldots,m_{Lh})$=augmented aerodynamic states. Similarly, formulations for other self-excited force and buffeting components can be obtained, but have been omitted here for the sake of brevity.

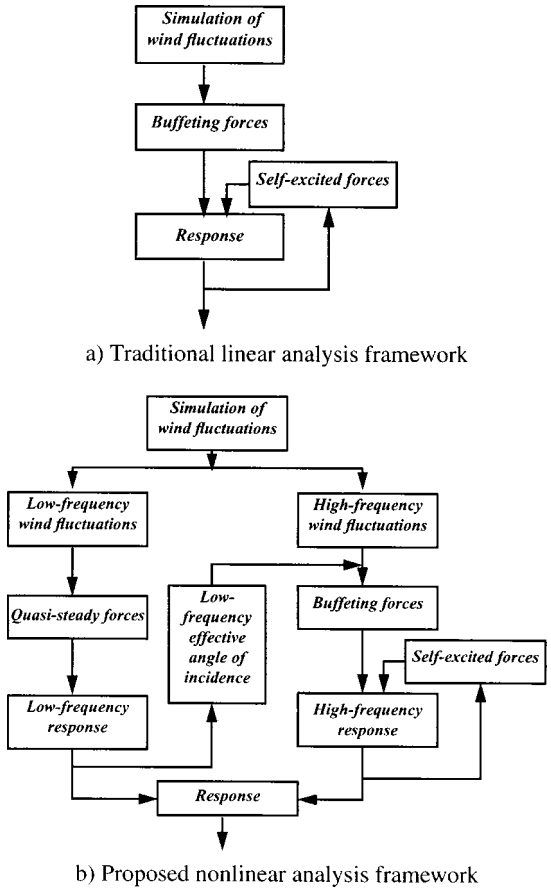

Fig. 2. Comparison between traditional linear and proposed nonlinear analysis frameworks (a) traditional linear analysis framework and (b) proposed nonlinear analysis framework

Nonlinear Aeroelastic Response Analysis

At a given mean wind velocity, the static deformation of the bridge is first calculated using a static analysis which is followed by a dynamic response analysis. The traditional linear and the proposed nonlinear analysis frameworks are shown schematically in Figs. 2(a and b). Using a multivariate autoregressive (AR) scheme (e.g., Chen et al. 2000b), the time histories of wind fluctuations at the centers of bridge elements with prescribed cross

power spectral density matrix are generated. The simulated wind fluctuations are subsequently separated into low-frequency and high-frequency components. The extraction of the low- and high-frequency components of the wind fluctuations is realized by a digital filter. The Newmark Beta step-by-step integration method is used for the dynamic response analysis. At each time step, the low-frequency components of response and effective angle of incidence are calculated which are then used to determine the aerodynamic characteristics for the calculation of high-frequency force components. An iterative calculation procedure is necessary for both the low-frequency and high-frequency responses, since the aerodynamic forces depend on the response. Although iterative calculation is required in this analysis, it converges quite rapidly. For most long span bridges, the low-frequency response is rather negligible, thus the effective angle of incidence can be simply evaluated from the low-frequency wind fluctuations [Eq. (7)].

Compared to traditional linear analysis utilizing linear aerodynamic forces as shown schematically in Fig. 2(a), the most important feature of the nonlinear framework is that the aerodynamic characteristics are modulated by the spatiotemporally varying low-frequency effective angle of incidence. Accordingly, the aeroelastic bridge system becomes time variant. Within this unique analysis framework, the effects of low-frequency components of turbulence on flutter and buffeting responses can be numerically investigated. The effects of turbulence on flutter are modeled through the changes in the effective angle of incidence caused by the turbulence and its influence on the self-excited forces and the flutter instability. Compared to the stochastic approach involving randomized dynamic pressure, which only includes the longitudinal wind fluctuations (e.g., Bucher and Lin 1988; and Lin and Li 1993), this nonlinear framework provides a more physically meaningful influence of turbulence. The basic representation of the nonlinear force model is similar to that proposed by Diana et al. (1995 and 1999), however, this model provides a clear insight to the relationship between the nonlinear and traditional linear force model, and presents a more efficient computational framework by way of invoking rational function approximation to take into account the frequency dependent aerodynamic characteristics, i.e., flutter derivatives, admittance functions, and spanwise coherence functions. The influence of the high-frequency component of turbulence is manifested in terms of changes in aerodynamic characteristics due to turbulence, which can be conveniently incorporated by employing aerodynamic characteristics derived in turbulent flows.

The consideration of structural nonlinearities is immediate in this time domain analysis framework. For linear structures, modal analysis techniques can be utilized to benefit from the reduction in computational effort by limiting the analysis to selected modes.

Structural Dynamic and Aerodynamic Characteristics

A three-span two-hinged suspension bridge with a main span of approximately 2,000 m was used to illustrate the proposed nonlinear analysis framework and to investigate the influence of nonlinear aerodynamics and turbulence on the bridge response. Generalized equations of motion in terms of the modal coordinates and consisting of the first 15 modes with natural frequencies ranging from 0.039 to 0.08 Hz were used to describe the bridge motion. The logarithmic decrement in each mode was assumed to be 0.02.

For simplicity and without loss of generality in modeling aerodynamic forces, only the aerodynamic forces acting on the bridge deck, which dominate the aeroelastic response of the bridge, were considered. The bridge deck was discretized into 70 elements in the spanwise direction. The aerodynamic characteristics of the proposed Messina Straits Bridge section were used with some modifications (Diana et al. 1995, 1999). The example bridge was assigned the static drag force coefficient of the Messina Bridge section, whereas the lift and pitching moment force coefficients including C_L, C_M, H_j^*, and A_j^* $(j=1,2,3,4)$ were set at four times the values of this section. Without these modifications, the analysis indicated that the critical flutter velocity of this example bridge was significantly high. This modification reduced the critical flutter velocity of the example bridge to within a meaningful range. Considering the sensitivity of aerodynamic force parameters with respect to the details of bridge section geometry, these adjustments are realistic for a modified bridge section. Accordingly, both static force coefficients and flutter derivatives for the lift and pitching moment were modified following the relationship between these two sets of force parameters. The self-excited drag force was evaluated based on quasi-steady theory, and only the component due to the lateral motion was included, i.e., $P_1^*=-2C_D/k$ and $P_j^*=0$ $(j=2,3,4,5,6)$.

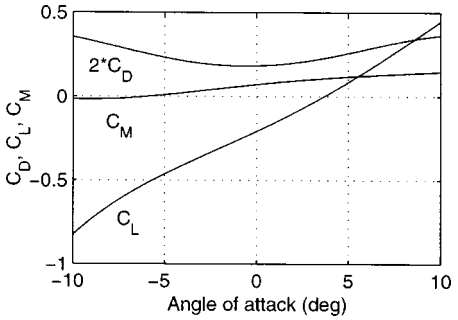

Fig. 3. Static force coefficients versus angle of attack

Fig. 3 shows the static force coefficients versus the angle of incidence. Fig. 4 shows the flutter derivatives H_3^* and A_2^* at dif-

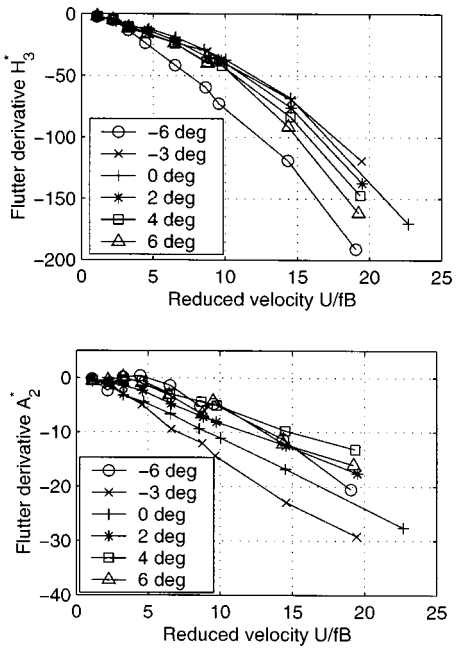

Fig. 4. Flutter derivatives H_3^* and A_2^* at varying angles of incidence

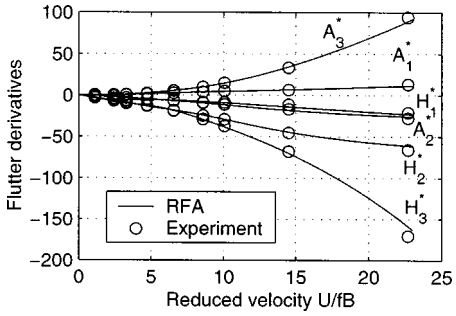

Fig. 5. Rational function approximation of flutter derivatives at angle of incidence of 0°

ferent angles of incidence. For each angle of incidence, the flutter derivatives were expressed in terms of a rational function approximation derived by a least squares curve-fitting of the experimental data. Since the experimental data was only available for a limited number of angles of incidence ranging between -6 and 6°, the corresponding values for intermediate angles of incidence were interpolated, and the values for angles larger than 6° or smaller than $-6°$ were assumed to be the same as 6 or $-6°$, respectively. As an example, the rational function approximation of $k^2(H_2^*+iH_3^*)$ at zero angle of incidence is given by

$$k^2(H_2^*+iH_3^*)=A_{L\alpha,1}+(ik)A_{L\alpha,2}+(ik)^2A_{L\alpha,3}+\sum_{j=1}^{m_{L\alpha}}\frac{(ik)A_{L\alpha,j+3}}{ik+d_{L\alpha,j}} \tag{21}$$

where $A_{L\alpha,1}=-3.4000$, $A_{L\alpha,2}=4.0586$, $A_{L\alpha,3}=0$, $A_{L\alpha,4}=7.2095$, $A_{L\alpha,5}=-55.9958$, $A_{L\alpha,6}=150.5695$, $A_{L\alpha,4}=-123.7077$, $d_{L\alpha,1}=0.2$, $d_{L\alpha,2}=0.4$, $d_{L\alpha,3}=0.6$, $d_{L\alpha,4}=0.8$, $m_{L\alpha}=4$, and, for example, the coefficient $A_{L\alpha,1}$ at a different angle of incidence, α, is given by

$$A_{L\alpha,1}=1.7359e+05\alpha^5-1.9096e+04\alpha^4-1.7452e+03\alpha^3+1.8687e+02\alpha^2+4.2932\alpha-3.4000 \tag{22}$$

Fig. 5 shows the comparison between the measured and fitted flutter derivatives. Results show an excellent agreement, which illustrates the accuracy of the rational function approximation.

The aerodynamic admittance and joint acceptance functions were considered invariant with respect to the angle of incidence for this example due to a lack of experimental data, although these features can be included in the proposed framework in a straightforward manner. Therefore, the nonlinearity in the buffeting forces was only introduced by the static force coefficients. The aerodynamic admittance functions for drag were described by the expressions given by Davenport, and for lift and pitching moment, were represented by the Sears function. The spanwise correlation of buffeting forces was assumed to be the same as the wind fluctuations in the approach flow. It is noted that more accurate modeling regarding the aerodynamic admittance functions and spanwise coherence functions can be immediately incorporated in the analysis when these are experimentally available. The von Kármán spectra was used for the simulation of wind fluctuations with the length scales of $L_u^x=L_u^y=80$ m and $L_w^x=L_w^y=40$ m, turbulence intensities of $\sigma_u/U=10\%$ and $\sigma_w/U=7.5\%$, and the decay factors of $\lambda_u=\lambda_w=8$ for the calculation of the coherence functions.

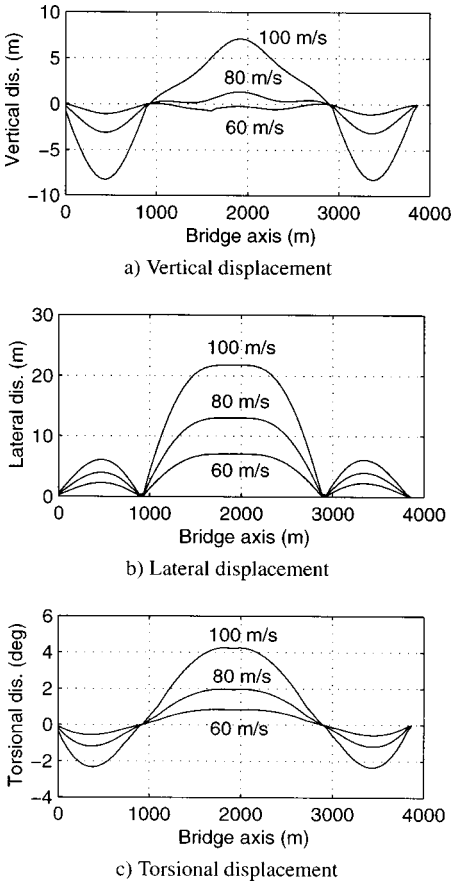

Fig. 6. Static deformation of bridge deck along bridge axis (a) vertical displacement, (b) lateral displacement, and (c) torsional displacement

Aerostatic Response Analysis

The response due to aerostatic forces was calculated at different mean wind velocities. The static torsional deformation of the bridge deck along the bridge axis at mean wind velocities of 60, 80, and 100 m/s is shown in Fig. 6. The bridge deck in the main span shows positive response angle, and exhibits large lateral deformation at high wind velocities. Fig. 7 shows the torsional deformation of the bridge deck at the midpoint of the main span as wind velocity increases. The torsional deformation of bridge deck increases significantly at wind velocities beyond 107 m/s. A di-

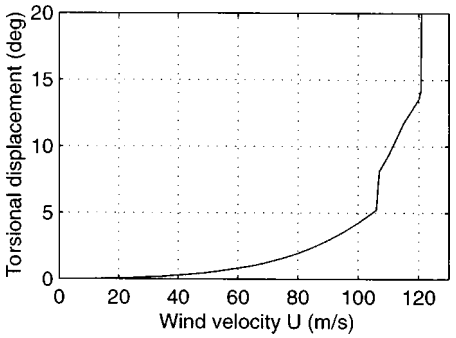

Fig. 7. Static torsional deformation of bridge deck at midpoint of main span

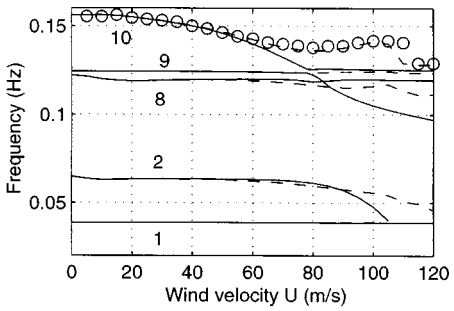

a) Frequency vs. wind velocity

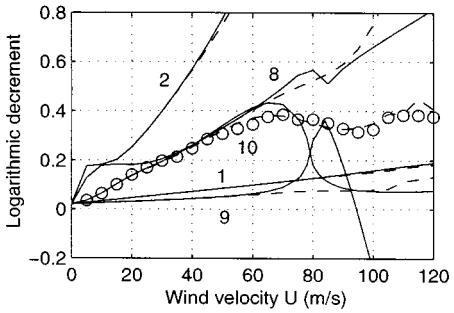

b) Damping ratio vs. wind velocity

Fig. 8. Influence of static rotation of bridge deck on aeroelastic modal properties (—— eigenvalue analysis, 0°; – – eigenvalue analysis, α_s; *o* time domain simulation, α_s) (a) frequency versus wind velocity and (b) damping ratio versus wind velocity

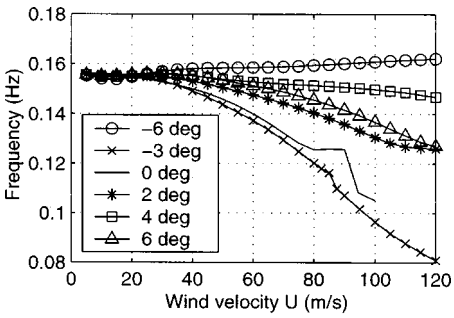

a) Frequency vs. wind velocity

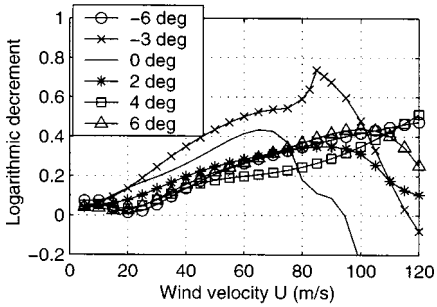

b) Damping ratio vs. wind velocity

Fig. 9. Influence of mean wind angle of incidence on modal properties of mode branch 10 (a) frequency versus wind velocity and (b) damping ratio versus wind velocity

vergence instability is observed at the wind velocity of 120.8 m/s beyond which the bridge becomes statically unstable.

Coupled Flutter Analysis

In order to examine the variations in the aeroelastic modal properties, i.e., the modal frequencies and damping ratios, with respect to the varying mean wind angles of incidence and wind velocities, a multimode coupled flutter analysis was conducted. In this analysis, linear self-excited forces were utilized and the solution of complex eigenvalue problems described by linear time invariant state-space representations with augmented aerodynamic states was sought. The lower 15 structural modes were considered in the analysis. The mean wind angles of incidence were kept constant along the span at -6, -3, 0, 2, 4, and 6°, as well as varied along the span following the static angle α_s.

Fig. 8 shows variations of the frequency and damping ratio of a number of important complex mode branches, i.e., mode branches 1, 2, 8, 9, and 10, with increasing wind velocity at mean wind angles of incidence of 0° and α_s. At zero wind velocity, these mode branches are the corresponding real-valued structural modes, where Modes 1 and 9 are the first and second symmetric lateral bending modes; Modes 2 and 8 are the first and second symmetric vertical bending modes; and Mode 10 is the first symmetric torsional mode. In the case of 0°, coupled flutter initiates at a wind velocity of 94.5 m/s. The curve veering of the frequency loci of the complex Mode Branches 9 and 10 is noted in the region of 80 m/s, which results in the switching of the two respective eigenmodes beyond this veering area. The curve veering phenomenon has been discussed in detail by Chen and Kareem (2003). For the case involving linearization of the self-excited forces at the static angle of the bridge, no flutter instability could be observed in the wind velocity range of up to 120 m/s. The static rotation of the bridge deck at high-wind velocities resulted in a significant influence on the modal damping of the torsional mode dominated branch. The frequency and damping ratio of Mode Branch 10 were also predicted through a time domain approach utilizing linear self-excited forces by simulating free vibration response (Chen et al. 2000b). The results are shown in Fig. 8 by circles. An excellent agreement between the complex eigenvalue analysis and the time domain simulation demonstrated the accuracy of the time domain modeling of the self-excited forces.

Fig. 9 shows variations of frequency and damping ratio of Mode Branch 10 with increasing wind velocity at different mean wind angles of incidence. At -3°, the critical flutter velocity is predicted to be 115.9 m/s, and no flutter is observed up to 120 m/s for other cases. Results clearly demonstrated the sensitivity of the aeroelastic modal properties with respect to changes in the mean wind angle of incidence on the flutter behavior.

Nonlinear Buffeting Response Analysis

The wind fluctuations at the center of each element along the bridge axis were simulated using a multivariate AR model for 2,400 s at 0.1 s increments. Ten sample realizations were generated and the corresponding buffeting responses were calculated. For each realization of response, the root-mean square (RMS) and maximum (MAX) responses were calculated and their mean values were estimated based on the simulated realizations. The analysis was conducted for the following cases using different aerodynamic force models: (1) linear self-excited and buffeting forces at zero angle of incidence; (2) linear self-excited and buf-

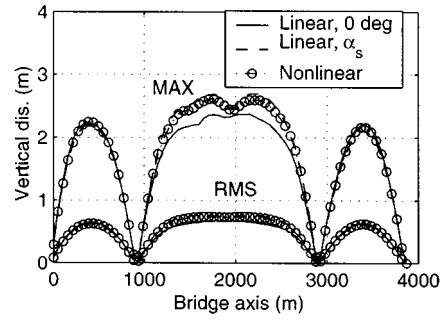

a) Vertical displacement

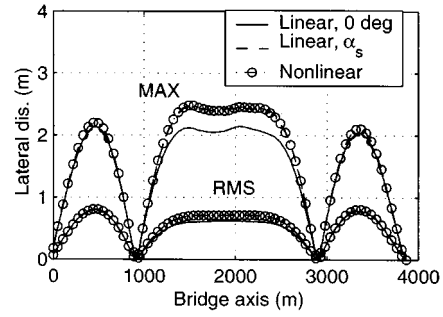

b) Lateral displacement

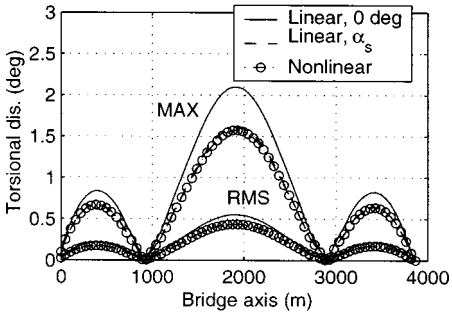

c) Torsional displacement

Fig. 10. Comparison of buffeting displacement of bridge deck ($U = 80$ m/s) (a) vertical displacement, (b) lateral displacement, and (c) torsional displacement

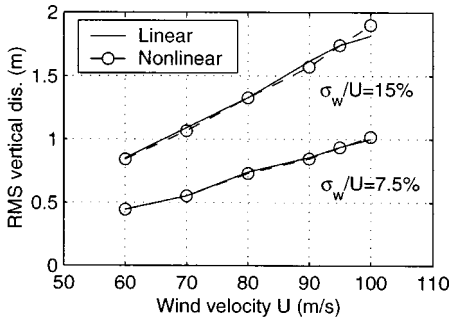

a) Vertical displacement

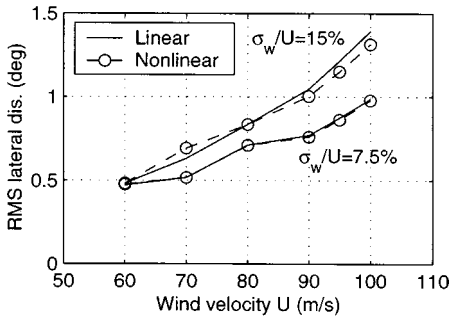

b) Lateral displacement

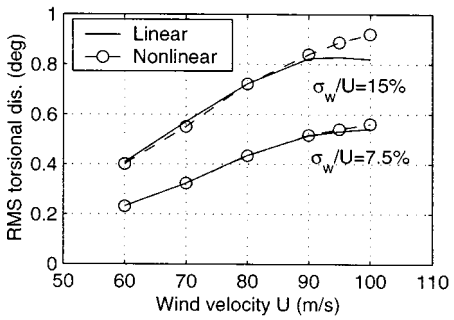

c) Torsional displacement

Fig. 11. Comparison of buffeting response of bridge deck at different wind velocities (a) vertical displacement, (b) lateral displacement, and (c) torsional displacement

feting forces at the static angle of the bridge; and (3) nonlinear self-excited and buffeting forces proposed in this study.

Fig. 10 shows a comparison of the RMS and MAX responses of the bridge deck in vertical, lateral, and torsional directions at the mean wind velocity of 80 m/s. Results illustrate the significance of including changes in the aerodynamic force characteristics, with respect to the static angle of the bridge deck, for accurately predicting the buffeting response. This feature becomes even more critical when the static rotation is remarkably large and the force characteristics are sensitive to changes in the mean angle of incidence. On the other hand, it is noted that the results from the nonlinear analysis are very close to the linear analysis based on the aerodynamic forces linearized at the statically deformed position of the bridge. The comparison of results at different mean wind velocities are shown in Fig. 11, which reinforces this observation. In the same figure, the results with a vertical turbulence intensity of 15% are also presented. It is noted that the influence of aerodynamic nonlinearities on the buffeting response is rather insignificant at low-wind velocities, however, at high-wind velocities the difference between the linear and nonlinear analyses clearly emerges.

Fig. 12 shows an example time history of the vertical wind fluctuation along with the associated low-frequency effective angle of incidence, as well as bridge lateral and torsional displacements at the midpoint of the main span at 80 m/s. In the same figure, the low-frequency effective angles of incidence at the quarter-point and three quarter-point of the main span are also plotted, which clearly underscore the spatiotemporal variations of low-frequency effective angle of incidence. The low-frequency effective angle of incidence due to wind fluctuations at the midpoint of the main span ranges between -2 and 2° with a net value between -0.3 and 3.97° including the static angle of 1.97°. The insensitivity of the aerodynamic nonlinearities to the buffeting response may be due to the fact that the modifications of the aerodynamic forces resulting from time dependent variations in the low-frequency effective angle of incidence did not consequently cause an apparent growth or decay of the response. This is in contrast with the cases of time invariant changes in the angle of incidence which permit sufficient time for the response to modify accordingly. Furthermore, the spatial variations of the low-frequency effective angles of incidence resulted in modifica-

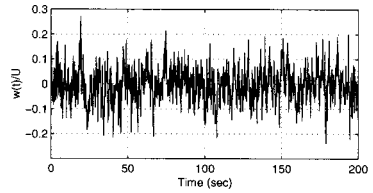

a) w-component of wind fluctuation

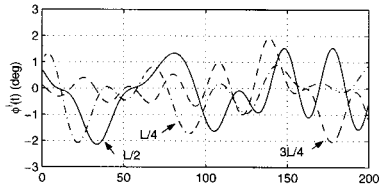

b) Low-frequency effective angle of incidence

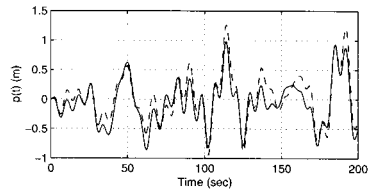

c) Lateral displacement (— Linear analysis; – – Nonlinear analysis)

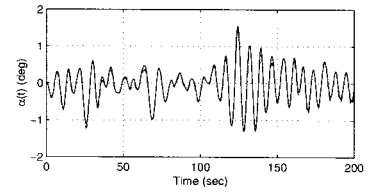

d) Torsional displacement (— Linear analysis; – – Nonlinear analysis)

Fig. 12. Time histories of wind fluctuation and buffeting response at midpoint of main span ($U=80$ m/s) (a) w-component of wind fluctuation, (b) low-frequency effective angle of incidence, (c) lateral displacement (—— linear analysis; – – nonlinear analysis), and (d) torsional displacement (—— linear analysis; – – nonlinear analysis)

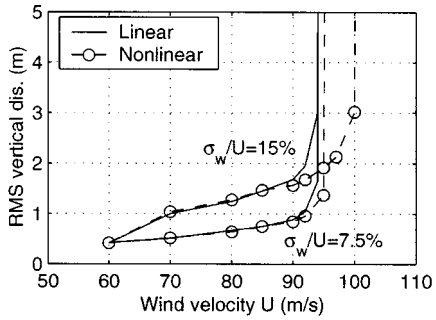

a) Vertical displacement

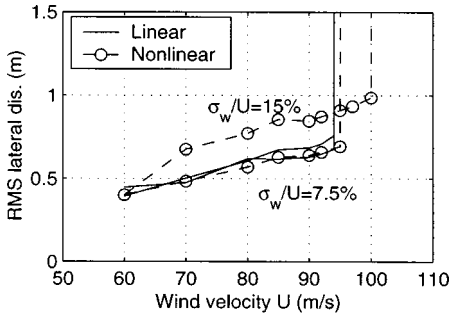

b) Lateral displacement

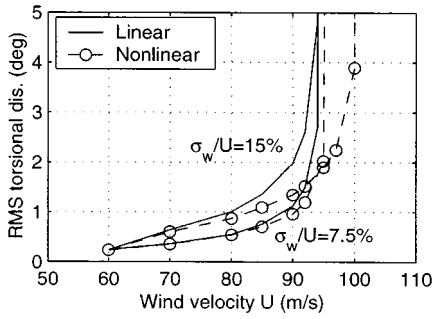

c) Torsional displacement

Fig. 13. Buffeting response of bridge deck neglecting static deformation (a) vertical displacement, (b) lateral displacement, and (c) torsional displacement

tions of the self-excited forces that varied along the span. In balance, this feature resulted in negating the overall contribution to the aerodynamic forces. As a result, the overall buffeting response was not substantially influenced by the nonlinearities, which lends support to the utility of the linear aerodynamic force model used in traditional analytical approaches.

It is noteworthy that the influence of aerodynamic nonlinearity depends on the level of the effective angle of incidence and the sensitivity of the force characteristics with respect to the effective angle of incidence. For the sake of comparison, the nonlinear analysis without the inclusion of the static angle in the effective angle of incidence was also conducted. The results were compared to those based on the linear analysis and are shown in Fig. 13. The linear buffeting response resulted in flutter instability beyond 94.5 m/s as predicted in the previous linear flutter analysis. At $\sigma_w/U=7.5\%$, a slight increase in the flutter boundary was observed in the nonlinear analysis, while the responses were close to those based on the linear analysis. At $\sigma_w/U=15\%$, the increase in the flutter boundary due to the nonlinear aerodynamic forces became quite distinct. While the linear analysis resulted in a distinct flutter boundary, the nonlinear analysis predicted a gradual growth in response with increasing wind velocity which is similar to the wind tunnel observations of full aeroelastic bridge models in turbulent flows (Irwin 1977). The influence of nonlinear aerodynamics on flutter is attributed to changes in the self-excited force characteristics that result from varying effective angle of incidence. This observation suggests that the experimentally observed turbulence effect on the flutter of full-bridges may in part be attributed to aerodynamic nonlinearities with respect to low-frequency wind fluctuations. The overall turbulence effects also include changes in aerodynamic characteristics due to turbulence which were not considered in the example study, but can be immediately included in the analysis when relevant data becomes available.

In Fig. 13(b), it is noted that the nonlinear analysis with $\sigma_w/U=15\%$ resulted in a higher-lateral response compared to the linear analysis. To gain a better understanding of this observation and to investigate the relative contributions of nonlinearities in the self-excited and buffeting forces, an analysis including only nonlinearities in the self-excited or buffeting forces was also conducted at 90 m/s. The results presented in Fig. 14 suggest that for vertical and torsional responses the influence of aerodynamic nonlinearities is mainly attributed to the nonlinear self-excited

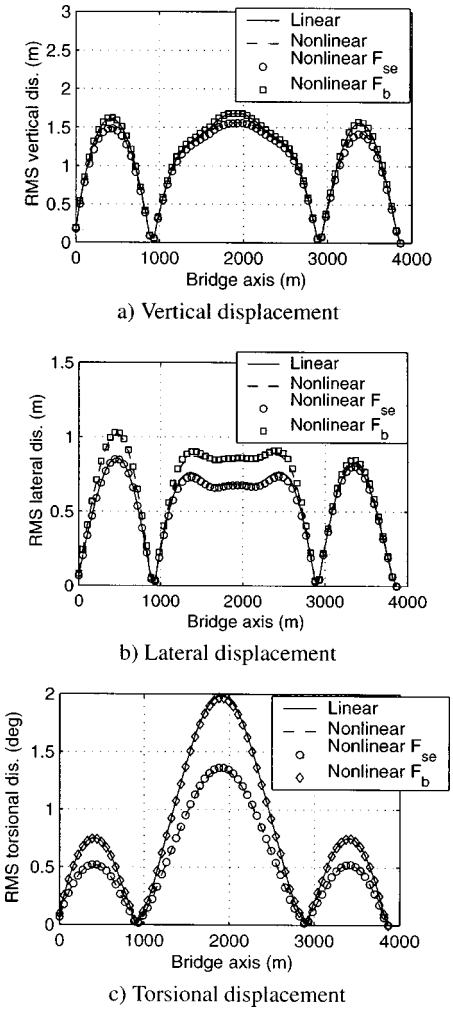

Fig. 14. Comparison of buffeting response at 90 m/s with $\sigma_w/U=15\%$, (a) vertical displacement, (b) lateral displacement, and (c) torsional displacement

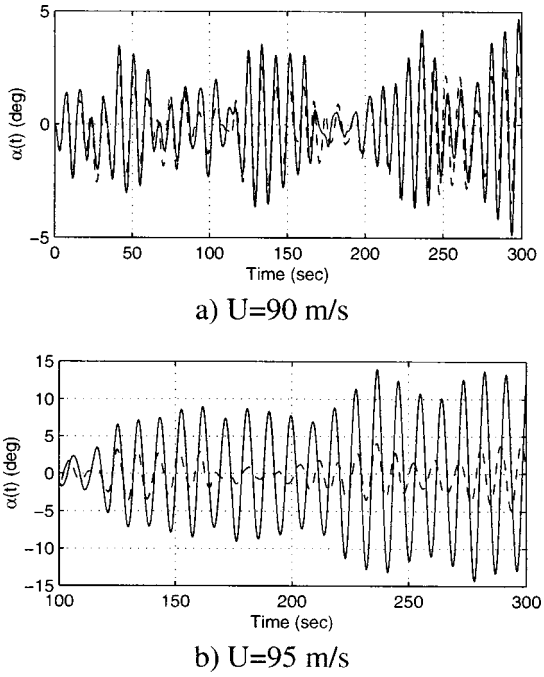

Fig. 15. Time histories of torsional displacement at midpoint of main span neglecting static deformation ($\sigma_w/U=15\%$, ——linear analysis; – – nonlinear analysis) (a) $U=90$ m/s and (b) $U=95$ m/s

forces, whereas for the lateral response it is due to the nonlinear buffeting forces, i.e., the variation of the drag coefficient at varying angles of incidence.

Fig. 15 shows time histories of the torsional displacement of the bridge deck at the midpoint of the main span using linear and nonlinear analysis at wind velocities of 90 and 95 m/s. The results clearly demonstrate the stabilizing effect of low-frequency turbulence on torsional response.

Concluding Remarks

A nonlinear aerodynamic force model and an associated time domain analysis framework were presented for estimating the aeroelastic response of bridges under turbulent winds. The most important feature of this nonlinear framework concerns the modulation of the aerodynamic force characteristics by the spatiotemporally varying low-frequency variations of the effective angle of incidence. The proposed analysis framework permits numerical study of the effects of low-frequency components of turbulence on flutter and buffeting response.

An application of this framework to a long span suspension bridge, with aerodynamic characteristics sensitive to the angle of incidence, was presented. Results demonstrated the significance of including the changes in the aerodynamic force characteristics, with respect to the static angle of the bridge deck, for accurately predicting the aeroelastic response. This feature becomes even more significant when the static rotation is remarkably large and the force characteristics are sensitive to the changes in the mean angle of incidence. On the other hand, the results pertaining to the long span suspension bridge example indicated that the modulation of force characteristics with low-frequency, spatiotemporally varying effective angle of incidence did not result in an apparent build up or decay of the response with inherent high-aeroelastic damping. As a result, the aerodynamic nonlinearities did not apparently influence the stable buffeting response which supports the efficacy of the linear aerodynamic force model used in traditional analytical approaches.

However, the aerodynamic nonlinearities, with respect to the low-frequency effective angles of incidence, may apparently influence the buffeting response with inherent low-aeroelastic damping and stabilize the flutter instability by deterring the buildup of response. While the linear analysis resulted in a distinct flutter boundary, the nonlinear analysis revealed a gradual growth in response with increasing wind velocity which is similar to the wind tunnel observations of full-aeroelastic bridge models in turbulent flows. This suggests that the effects of turbulence on the flutter of full-bridges may in part be attributed to aerodynamic nonlinearities, i.e., nonlinearities in the self-excited forces. The overall turbulence effects also include changes in aerodynamic characteristics due to turbulence, which were not included in the studied example, but can be incorporated immediately in the analysis when related data becomes available.

A coordinated experimental investigation is planned for further validation of the proposed approach. This effort seeks an improved understanding of the turbulence induced modifications of the magnitudes and spanwise coherence of both the buffeting and the self-excited forces. Incorporating such work with measure-

ments of the effective angle and amplitude dependence of the aerodynamic forces will provide an experimental foundation for the proposed analysis work.

The writers would like to underscore that the proposed analysis framework is one of a few initial attempts to address the next frontier of bridge aerodynamics, i.e., the challenge of modeling nonlinearity and turbulence in aeroelastic response of bridges. While this study provides an effective analysis framework, additional follow-up studies like those which have followed the early development of linear bridge aeroelastic analysis would help to further refine or validate this approach.

Acknowledgment

The support for this work was provided in part by NSF Grant No. CMS 95-03779. This support is gratefully acknowledged.

References

Bucher, C. G., and Lin, Y. K. (1988). ''Stochastic stability of bridges considering coupled modes.'' *J. Eng. Mech.,* 114(12), 2055–2071.

Chen, X., and Kareem, A. (2001a). ''Aeroelastic analysis of bridges under multi-correlated winds: Integrated state-space approach.'' *J. Eng. Mech.,* 127(11), 1124–1134.

Chen, X., and Kareem, A. (2001b). ''Nonlinear response analysis of long-span bridge under turbulent winds.'' *J. Wind. Eng. Ind. Aerodyn.,* 89(14–15), 1335–1350.

Chen, X., and Kareem, A. (2002). ''Advances in modeling of aerodynamic forces on bridge decks.'' *J. Eng. Mech.,* 128(11), 1193–1205.

Chen, X., and Kareem, A. (2003). ''Curve veering of eigenvalue loci of bridges with aeroelastic effects.'' *J. Eng. Mech.,* 129(2), 146–159.

Chen, X., Kareem, A., and Matsumoto, M. (2001). ''Muitimode coupled flutter and buffeting analysis of long-span bridges.'' *J. Wind. Eng. Ind. Aerodyn.,* 89(7–8), 649–664.

Chen, X., Matsumoto, M., and Kareem, A. (2000a). ''Aerodynamic coupling effects on flutter and buffeting of bridges.'' *J. Eng. Mech.,* 126(1), 17–26.

Chen, X., Matsumoto, M., and Kareem, A. (2000b). ''Time domain flutter and buffeting response analysis of bridges.'' *J. Eng. Mech.,* 126(1), 7–16.

Davenport, A. G. (1962). ''Buffeting of a suspension bridge by stormy winds.'' *J. Struct. Eng.,* 88(ST3), 233–268.

Davenport, A. G., and King, J. P. C. (1993). ''The influence of topography and storm structure on long span bridge behavior in wind.'' *Int. Seminar on Utilization of Large Boundary Layer Wind Tunnels*, Public Works Institute, Japan, 11–21.

Davenport, A. G., King, J. P. C., and Larose, G. (1992). ''Taut strip model tests.'' *Aerodynamics of large bridges*, A. Larsen, ed., Balkema, Rotterdam, The Netherlands, 113–124.

Diana, G., Cheli, F., Zasso, A., and Bocciolone, M. (1999). ''Suspension bridge response to turbulent wind: Comparison of new numerical simulation method results with full scale data.'' *Proc., 10th Int. Conf. on Wind Eng., Wind Eng. into the 21 Century*, A. Larsen, G. L. Larose, and F. M. Livesey, eds., Balkema, Rotterdam, The Netherlands, 871–878.

Diana, G., Falco, M., Bruni, S., Cigada, A., Larose, G. L., Damsgaard, A., and Collina, A. (1995). ''Comparisons between wind tunnel tests on a full aeroelastic model of the proposed bridge over Stretto di Messina and numerical results.'' *J. Wind. Eng. Ind. Aerodyn.,* 54/55, 101–113.

Haan, F. L., Kareem, A., and Szewczyk, A. A. (2000). ''Experimental measurements of spanwise correlation of self-excited forces on a rectangular cross section.'' *Volume of Abstracts, 4th Int. Colloquium on Bluff Body Aerodynamics and Applications (BBAA IV)*, Ruhr-Univ., Bochum, Germany, 439–442.

Irwin, H. P. A. H. (1977). ''Wind tunnel and analytical investigation of the response of Lions Gate Bridge to turbulent wind.'' *NAE-LTR-LA-210*, National Resource Council (NRC) of Canada, Québec.

Jones, N. P., Scanlan, R. H., Jain A., and Katsuchi, H. (1998). ''Advances (and challenges) in the prediction of long-span bridge response to wind.'' *Bridge aerodynamics*, A. Larsen and S. Esdahl, eds., Balkema, Rotterdam, The Netherlands, 59–85.

Katsuchi, H., Jones, N. P., and Scanlan, R. H. (1999). ''Multimode coupled flutter and buffeting analysis of the Akashi-Kaikyo Bridge.'' *J. Struct. Eng.,* 125(1), 60–70.

Kovacs, I., Svensson, H. S., and Jordet, E. (1992). ''Analytical aerodynamic investigation of cable-stayed helgeland bridge.'' *J. Struct. Eng.,* 118(1), 147–168.

Larose, G. L., and Mann, J. (1998). ''Gust loading on streamlined bridge decks.'' *J. Fluids Struct.,* 12, 511–536.

Lin, Y. K., and Li, Q. C. (1993). ''New stochastic theory for bridge stability in turbulent flow.'' *J. Eng. Mech.,* 119(1), 113–127.

Matsumoto, M. (1999). ''Recent study on bluff body aerodynamics and its mechanism.'' *Proc., 10th Int. Conf. on Wind Engineering, Wind Engineering into the 21st Century*, A. Larsen, G. L. Larose, and F. M. Livesey, eds., Balkema, Rotterdam, The Netherlands, 67–78.

Matsumoto, M., Yagi, T., Ishizaki, H., Shitato, H., and Chen, X. (1998). ''Aerodynamic stability of 2-edge girders for cable-stayed bridge.'' *Proc., 15th National Symp. on Wind Engineering*, Japan Association for Wind Engineering, Tokyo, 389–394 (in Japanese).

Miyata, T., Yamada, H., Boonyapinyo, V., and Stantos, J. C. (1995). ''Analytical investigation on the response of a very long suspension bridge under gusty wind.'' *Proc., 9th Int. Conf. on Wind Engineering* (ICWE), New Delhi, India, 1006–1017.

Nakamura, Y. (1993). ''Bluff-body aerodynamics and turbulence.'' *J. Wind. Eng. Ind. Aerodyn.,* 49, 65–78.

Sakar, P. P., Jones, N. P., and Scanlan, R. H. (1994). ''Identification of aeroelastic parameters of flexible bridges.'' *J. Eng. Mech.,* 120(8), 1718–1742.

Scanlan, R. H. (1978). ''The action of flexible bridges under wind. 1: Flutter theory; 2: Buffeting theory.'' *J. Sound Vib.,* 60(2), 187–211.

Scanlan, R. H. (1993). ''Problematics in formulation of wind-force models for bridge decks.'' *J. Eng. Mech.,* 119(7), 1353–1375.

Scanlan, R. H. (1997). ''Amplitude and turbulence effects on bridge flutter derivatives.'' *J. Struct. Eng.,* 123(2), 232–236.

Scanlan, R. H., and Lin, W.-H. (1978). ''Effects of turbulence on bridge flutter derivatives.'' *J. Eng. Mech. Div., Am. Soc. Civ. Eng.,* 104(4), 719–733.

van Oudheusden, B. W. (2000). ''Aerodynamic stiffness and damping effects in the rotational galloping of a rectangular cross-section.'' *J. Fluids Struct.,* 14, 1119–1144.

Walshe, D. E., and Wyatt, T. A. (1983). ''Measurement and application of the aerodynamic admittance function for a box-girder bridge.'' *J. Wind. Eng. Ind. Aerodyn.,* 14, 211–222.

Xu, Y. L., Sun, D. K., Ko, J. M., and Lin, J. H. (2000). ''Fully coupled buffeting analysis of Tsing Ma suspension bridge.'' *J. Wind. Eng. Ind. Aerodyn.,* 85(1), 97–117.

Zasso, A., and Curami, A. (1993). ''Extensive identification of bridge deck aeroelastic coefficient: Average angle of attack, Reynolds number and other parameters effects.'' *Proc., 3rd Asian Pacific Symp. on Wind Engineering*, Univ. of Hong Kong, Hong Kong, 143–148.